ISSN: 0067-2904

Removing Cobalt ions from Industrial Wastewater Using Chitosan

Hakim H. Kadhim*, Khulood A. Saleh
Department of Chemistry, College of Science, University of Baghdad, Baghdad, Iraq

Received: 9/6/2021 Accepted: 4/11/2021 Published: 30/8/2022

Abstract

In batch experiments, a natural chitosan adsorbent was employed to extract cobalt ions from industrial wastewater under varied parameters of starting concentration, adsorbent weight, pH, and contact duration. The adsorbent was examined using FTIR, XRD, and AFM. For an initial cobalt ion concentration of $5x10^{-2}$ mol/l at pH 6, time 35 minutes, temperature 25 °C, and adsorbing dose 0.1 g, the results showed a maximum removal percentage of 99.0 percent. The Freundlich isotherm and the pseudo-second order kinetic model both suit the experimental data well. According to thermodynamic studies, the process was spontaneous and endothermic.

Keywords: Chitosan, Adsorption, Cobalt, Kinetic, Thermodynamic.

إزالة أيونات الكوبالت من مياه الصرف الصناعي باستخدام الشيتوزان

حكيم حيال كاظم, خلود عبد صالح
قسم الكيمياء, كلية العلوم, جامعة بغداد, بغداد, العراق

الخلاصة

مادة مازة طبيعية الشيتوزان تم استخدامها في التجارب على دفعات لإزالة ايونات الكوبالت من مياه الصرف الصناعي في ظل ظروف مختلفة من التركيز الأولي, وزن المادة المازة, درجة الحموضة ووقت التلامس. تم استخدام FTIR , XRD و AFM لفحص المادة المازة. نسبة الازالة القصوى تساوي % 99.0 لتركيز أيون الكوبالت الأولي $5x10^{-2}$ مول / لتر عند الأس الهيدروجيني 6 ،الوقت 35 دقيقة، درجة الحرارة 25 درجة مئوية وجرعة الامتزاز 0.1 غرام. تتناسب النتائج التجريبية مع النموذج الحركي من المرتبة الثانية الكاذبة ومع نموذج متساوي درجة الحرارة فريندلش. كانت العملية تلقائية وماصة للحرارة، وفقاً لدراسات الثرموديناميك.

1. Introduction

Wastewater, which is a mixture of liquid and solid pollutants that results from the use of water in households, factories, and commercial establishments [1], is a major source of environmental pollution. Electroplating, electrolysis, coatings, textiles, insecticides, medicines, papermaking, printing, dyeing, and other chemical industries have all wreaked havoc on the environment [2]. Cobalt is a natural element (atomic number 27) that ranks 24th on the list of the richest heavy metals in the Earth's crust. While cobalt exists in three oxidation states (0, +2, and +3), +2 is the most common oxidation state in the environment

*Email: hhk92.hh@gmail.com

[3]. Cobalt is a ferromagnetic metal used in a variety of industrial applications, including the production of stainless and superalloys for parts for gas turbine engines, magnets and magnetic recording media, petroleum catalysts, and chemical industries [4]. Vitamin B12, which is required for brain and nervous system function as well as blood production, contains cobalt as a key cofactor. Excessive Co intake, on the other hand, may be detrimental to both people and cattle. High levels of this component can induce harmful consequences such as nausea, high blood pressure (hypertension), reproductive issues, high blood sugar (hyperglycemia), lung illness, and bone deformities, as well as possibly cause living cell mutations (genetic alterations) [5-9]. Acute toxicity to the plant kingdom can also be caused by a large amount of Co in the soil [10]. In live-stock irrigation and irrigation water, the allowable limits of Co (II) are 1.0 and 0.05 mg/l, respectively (Environmental Bureau of Investigation, Canadian Water Quality Guidelines). The maximum allowable concentration of cobalt (II) in drinking water is 0.05 mg/l, according to the World Health Organization (WHO) [11]. Several methods for removing heavy metals from wastewater have been investigated over the last decade, including adsorption, precipitation, ion exchange, membrane process, electrocoagulation, and electrodeposition [12-14]. Among the above mentioned methods, adsorption has inherent benefits such as low cost, high removal rate, ease of access, and less secondary pollution [15]. Different types of natural adsorbents are used for removal of metal ions from wastewater. Chitosan (CS) is a substance derived primarily from chitin, a carbohydrate found in the outer shells of seafood such as shrimp and crustaceans [16,17]. CS is an inexpensive bio-sorbent and disinfectant and has many advantages such as the amino functional group, which perfectly interacts between metal ions, biodegradability, bio-compatibility, and their non-toxic behavior [18].

We investigate the effectiveness of chitosan for removing cobalt from industrial wastewater under a variety of circumstances, including pH, starting concentration, adsorbent dosage, and contact duration. Langmuir and Freundlich isothermal adsorption were used to test the adsorption results, and thermodynamic parameters were determined as well. A pseudo-first order and pseudo-second order equations are used to examine the kinetic data.

2. Materials and methods

2.1. Materials

Chitosan $C_{56}H_{103}N_9O_{39}$ (≥ 90% deacetylation) were supplied by Cheng Du Micxy Chemical Co., Ltd (Cheng Du, China). Cobalt chloride hexahydrate, Hydrochloric acid, Sodium hydroxide were supplied by BDH.

2.2. Characterization

The FTIR spectrum of CS was measured by using a Shimadzu IRAffinity-1 FTIR Spectrophotometer (Shimadzu Corp., Japan). The spectral scan ranged between 400 and 4000 cm^{-1}. The X-ray diffraction (XRD) pattern of chitosan was studied using a Shimadzu XRD-6000 X-ray diffractometer (Shimadzu, Japan) in the 5–80° (2θ) range with Cu Kα (λ=1.5406 A^o), worked at 100 mA and 40KV. To get a quantitative picture of grain size and surface roughness of chitosan, atomic force microscope (AFM) (SPM AA3000 Angstrom Advanced Inc, USA) was applied.

2.3. Adsorption experiments

The stock solution of Cobalt chloride hexahydrate ($CoCl_2.6H_2O$) 0.1 (mol/l) was prepared by dissolving 11.89 g of Cobalt chloride in 500 ml of distilled water and then dilute to required concentration. Adsorption experiments were carried out in a batch model using a Cobalt chloride (50 ml) solution in a series of conical flasks (250 ml) at starting concentrations ranging from $5x10^{-2}$ to $1x10^{-4}$ mol/l. For pH adjustment, HCl (0.1M) and NaOH (0.1M) solutions were used. To achieve equilibrium, 0.1 g of CS powder was added to cobalt solution and stirred constantly for 35 min. After centrifuging the mixture for 5 min, the amount of cobalt adsorbed was determined using an atomic absorption spectrophotometer

(AAS) (Model: AA-7000, Shimadzu). Equations were used to measure the cobalt removal percentage and equilibrium uptake [19]:

$$\%Removal = \frac{C_o - C_e}{C_o}\ 100 (1)$$

$$q_e = \frac{C_o - C_e}{M} V (2)$$

Where, C_o is the initial concentration (mol/l), M (g) adsorbent weight, C_e is equilibrium concentration (mol/l), and V the volume of the solution in liters.

3. Results and Discussion

3.1. Characterization study

Figure 1 depicts the FTIR spectrum of CS. A broad band appears in the CS spectrum at 3441.01 cm^{-1}, which corresponds to the stretching vibrations of the N-H and O-H groups. A peak at 2889.37 cm^{-1} can be characterized for C-H extending the aliphatic group's vibration. The C=O stretching vibration (amide I band) and C-N stretching vibration (amide III band) in amide groups are represented by the absorption bands at 1654.92 cm^{-1} and 1379.1 cm^{-1}, respectively. The N-H bending vibration and N-H deformation vibration occurs at 1597.06 cm^{-1} and 1421.54 cm^{-1} in the primary amine groups ($-NH_2$). Other significant absorption bands in CS can be found at 1323.17 cm^{-1} (C-N stretching vibration), 1153.43 cm^{-1} (anti-symmetrical stretching vibration of the C-O-C bridge), 1072.42 cm^{-1} (C-O stretching vibration of a saccharide structure), and 1031.92 cm^{-1} (O-H bending vibration) [20].

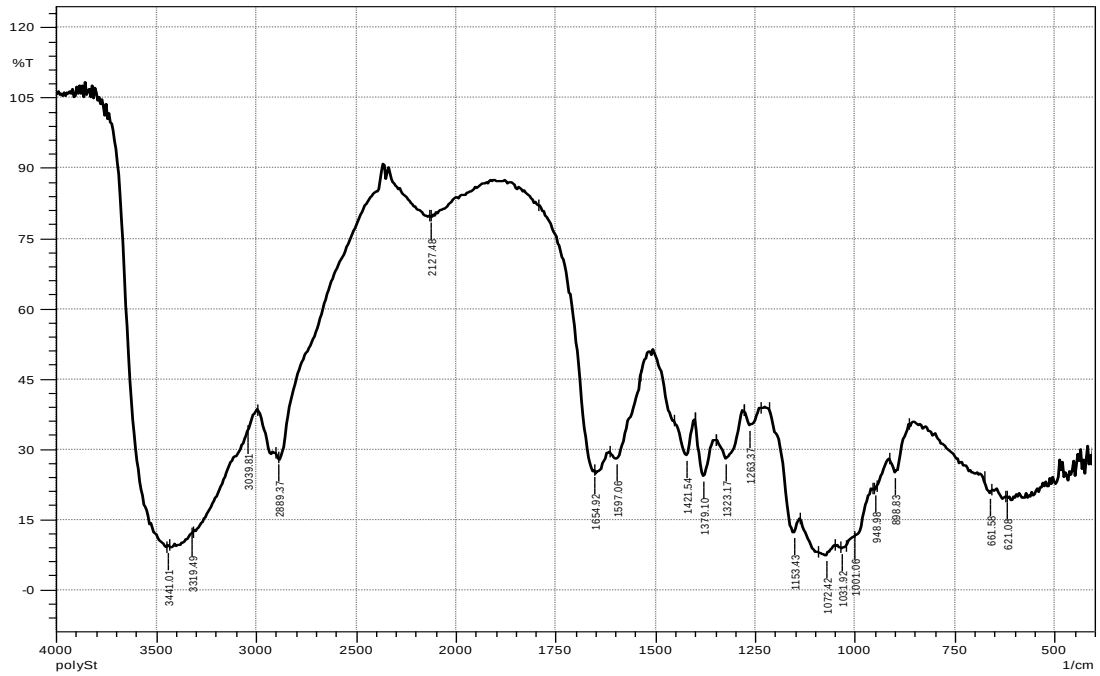

Figure 1- FTIR spectrum of CS

Figure 2 shows the XRD pattern of the chitosan sample. The characteristic peaks of chitosan located at 2θ =12.3^o and 20.2^o(JCPDS card No. 039– 1894) corresponding to diffraction from (002) and (101) planes respectively for Orthorhombic structure as illustrated by Santa et al.[21] and Okuyamaet al. (1997) [22]. The appearance of the broad peak at 20.2^o was interpreted by the previous researchers as a result of the arrangement of the chitosan chains in the form of parallel planes to give the orthorhombic form [23], or interpreted as a polymorphic form [24].

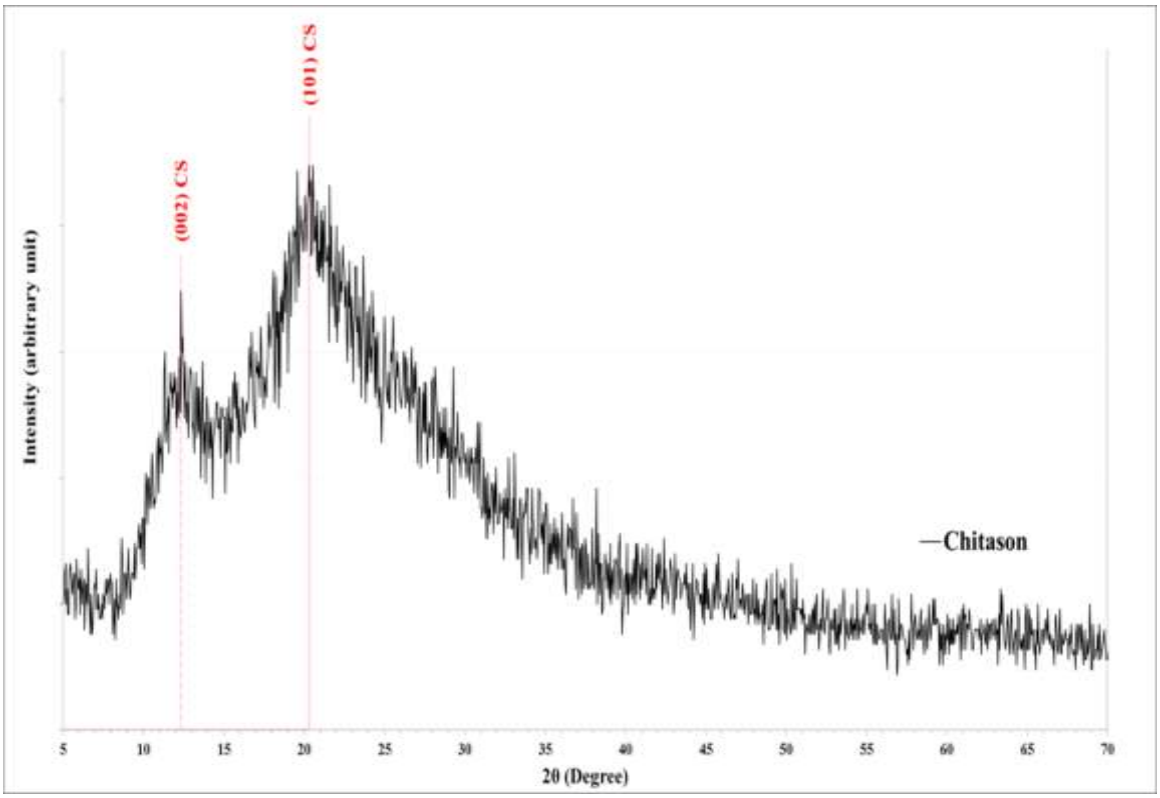

Figure 2-XRD pattern for chitosan

Figure 3 shows typical images of AFM surface (3D and 2D), and Table 2 shows the granularity cumulating distribution of Chitosan. The average diameter was (80.72) nm.

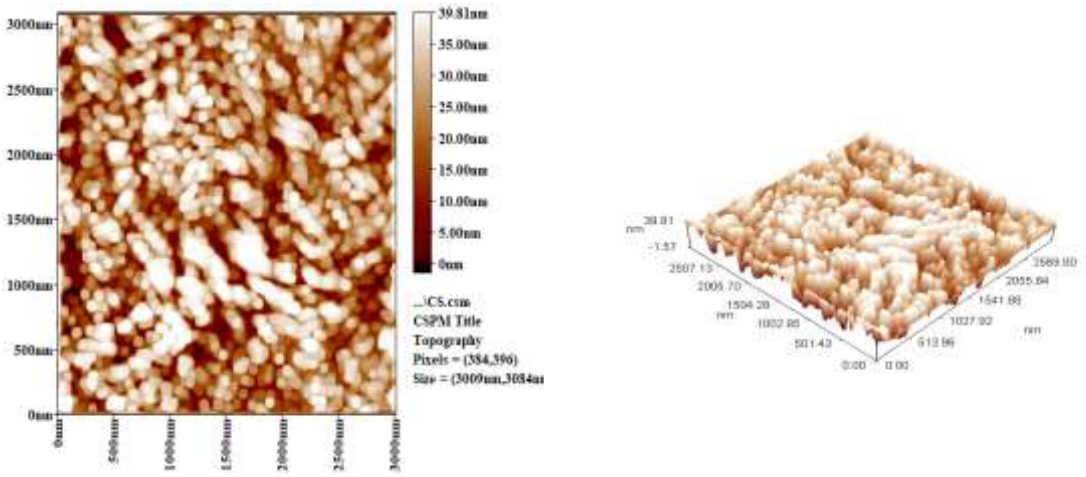

Figure 3- AFM images for Chitosan

Table 1- Granularity cumulating distribution & average diameter for Chitosan

Avg. Diameter:80.72 nm			**<=10% Diameter:**45.00 nm					
<=50% Diameter:75.00 nm			**<=90% Diameter:**115.00 nm					
Diameter (nm)<	**Volume (%)**	**Cumulation (%)**	**Diameter (nm)<**	**Volume (%)**	**Cumulation (%)**	**Diameter (nm)<**	**Volume (%)**	**Cumulation (%)**
20.00	0.21	0.21	70.00	6.61	40.09			
30.00	1.28	1.49	75.00	4.26	44.35	115.00	4.69	87.63
35.00	1.92	3.41	80.00	6.82	51.17	120.00	2.99	90.62
40.00	2.56	5.97	85.00	7.04	58.21	125.00	2.35	92.96
45.00	2.13	8.10	90.00	4.48	62.69	130.00	2.99	95.95
50.00	4.90	13.01	95.00	6.82	69.51	135.00	1.71	97.65
55.00	4.69	17.70	100.00	4.26	73.77	140.00	1.49	99.15
60.00	8.32	26.01	105.00	5.33	79.10	145.00	0.85	100.00
65.00	7.46	33.48	110.00	3.84	82.94			

3.2. Effect of contact time

The effect of contact time between the CS and Co (II) on the removal percentage was determined at $5x10^{-4}$ mol/l initial Co (II) concentration, 0.1g adsorbent weight, and 298K. Figure 4 shows the removal % rising over time, with the amount of Co (II) adsorbed on the adsorbent equaling the amount of Co (II) desorbed from the adsorbent after 35 minutes.

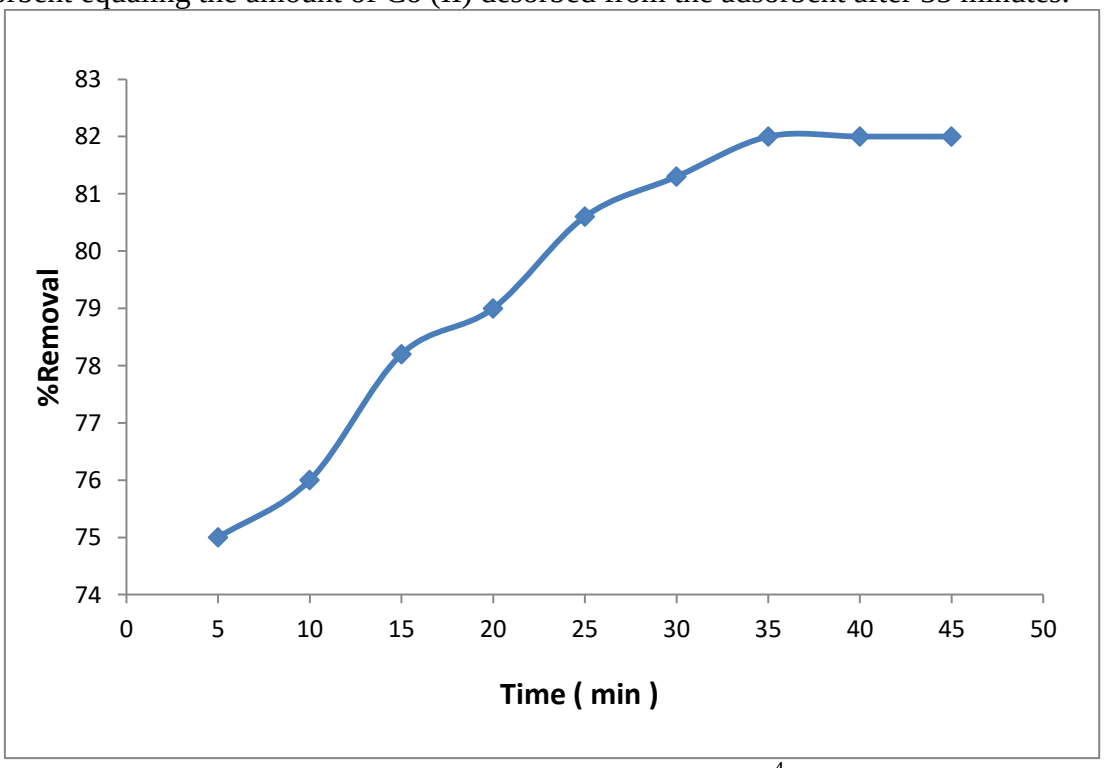

Figure 4- Effect of contact time on percentage removal of $5x10^{-4}$ mol/l Co (II) at 298K.

3.3. Effect of adsorbent weight

By adjusting the weight of CS in 50 ml of $5x10^{-4}$ mol/l cobalt solution from 0.05 g to 0.25 g, the effect of different CS weights on the ratio of Co(II) removal at 35 min contact time was examined. Figure 5 demonstrates that when the weight of CS increases, the percentage of removal increases because more adsorbent sites are created, and bigger surface area indicates more adsorbent sites [25, 26].

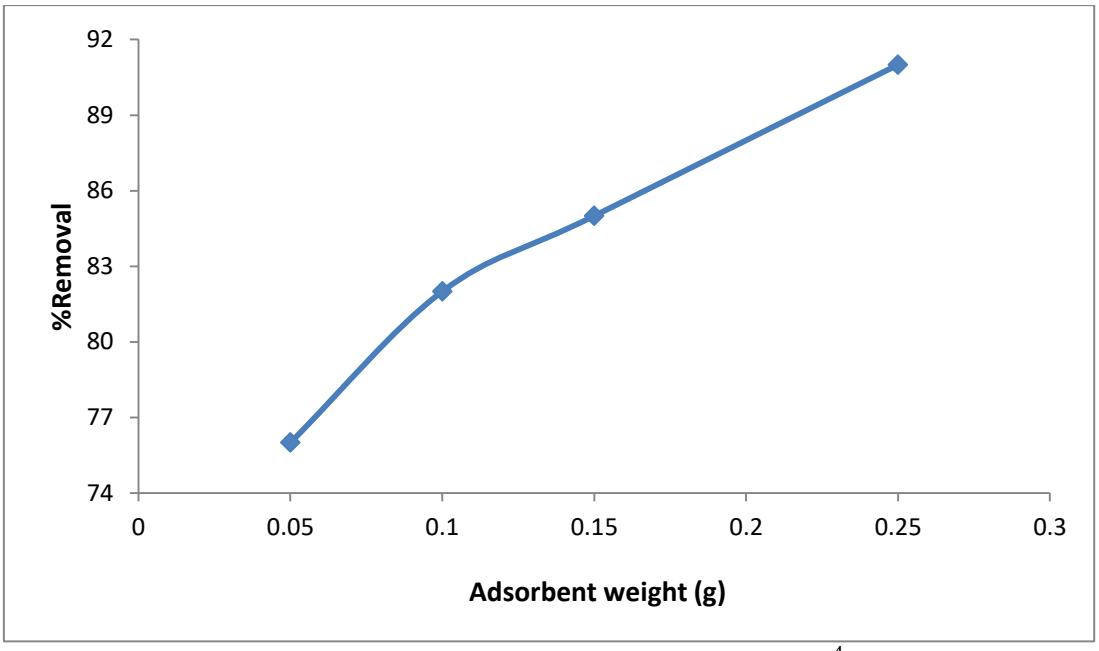

Figure 5- Effect of adsorbent weight on percentage removal of $5x10^{-4}$ mol/l Co (II) at 298 K.

3.4. Effect of initial concentration

To demonstrate the effect of the initial Co (II) concentration, different concentrations ($1x10^{-4}$, $5x10^{-4}$, $1x10^{-3}$, $5x10^{-3}$, $1x10^{-2}$ and $5x10^{-2}$) mol/l were used at 298K, adsorbent weight (0.1 g), and shaking period 35 min. Figure 6 shows that when the initial Co (II) concentration increased, the removal efficiency is also increased. At a low concentration, the ratio of number of active sites that available per unit Co (II) concentration was a small may be due to increased competition for active sites [27]. As a result, the adsorption became unaffected by the starting concentration. The contact forces, which are important for overcoming the barrier to mass transfer between Co (II) and the CS, increase as the initial Co (II) concentration rises [28]. The majority of the active sites got occupied as the initial Co (II) concentration rose, resulting in a small improvement in removal efficiency.

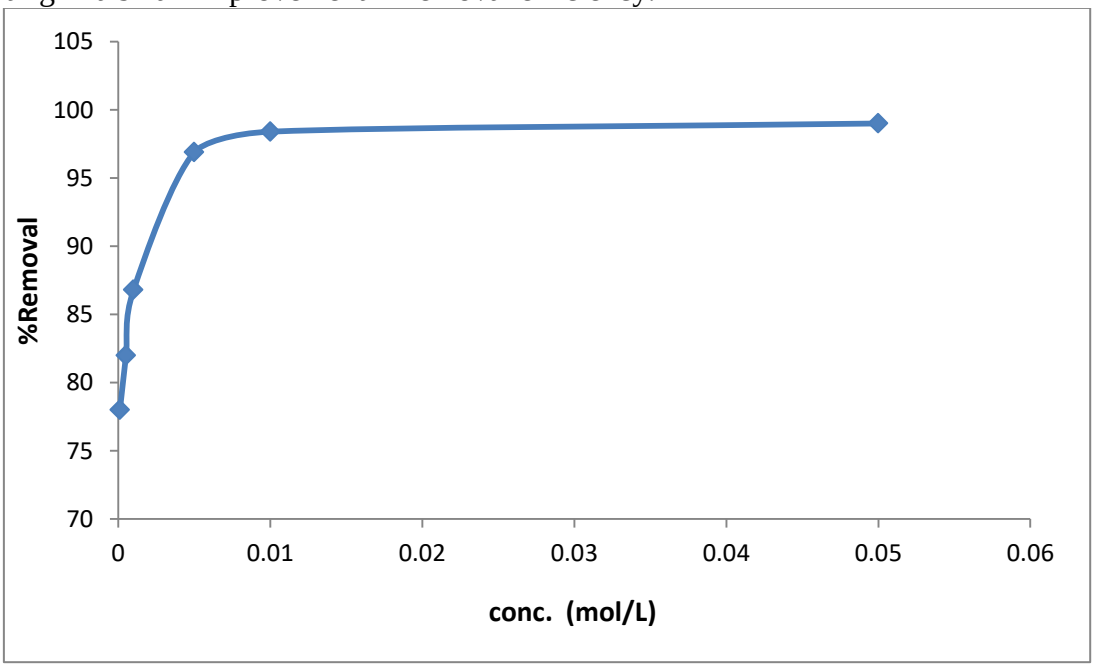

Figure 6- Effect of initial concentration on percentage removal of Co (II) at 298K.

According to Figure 6, the optimal concentration of Co(II) is $5x10^{-2}$ mol/l, so it will be used to study the effect of pH**.**

3.5. Effect of pH

The electric charge of the adsorbent surface, as well as the ionic geometries of the adsorbent molecule, were affected by the pH of the solution. As a result, the adsorption of Co (II) rises as the acidity lowers, since the hydrogen ion competes with the Co (II) molecule in an acid media, and as the quantity of hydrogen ions drops, more adsorption sites become accessible to adsorb Co (II) [25]. The optimal pH, as shown in Figure 7, is 6. Adsorption studies could not be performed at pH values greater than 6 due to $Co(OH)_2$ precipitation.

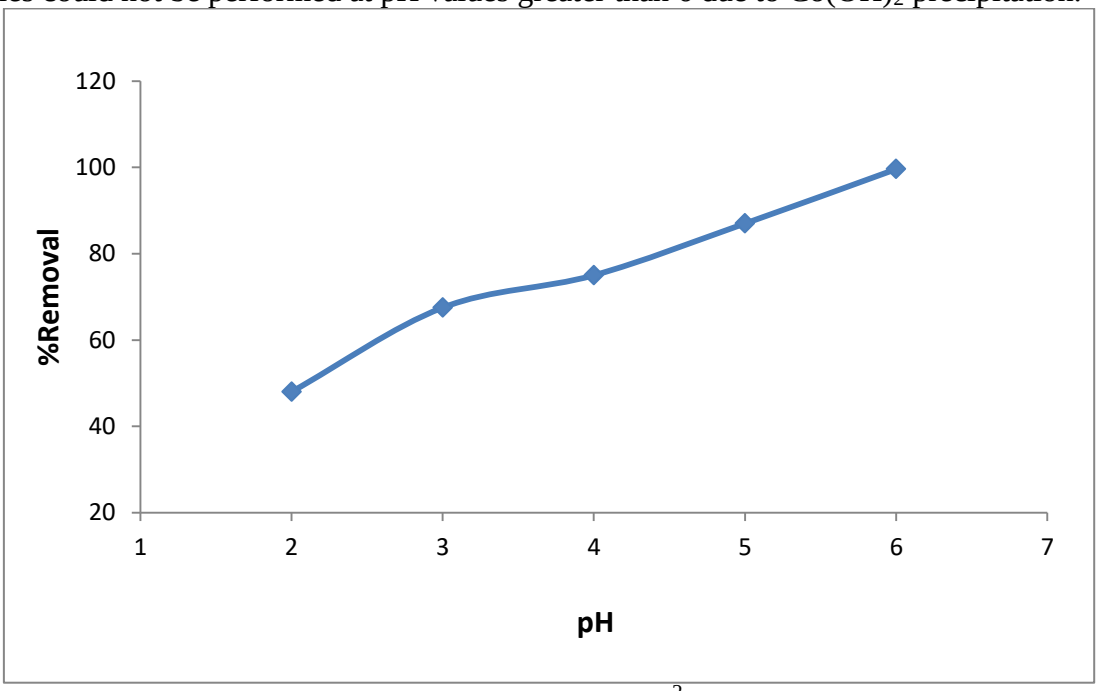

Figure 7- Effect of pH on percentage removal of $5x10^{-2}$ mol/l optimum concentration of Co (II) at 298K.

3.6. Equilibrium isotherm

The isotherm of adsorption describes the relation between the number of Co (II) molecules adsorbed by adsorbent mass and their balance at a constant temperature. Adsorption isotherms are essential for the design of any adsorption system. The isotherms were investigated using 50 ml of cobalt solution at various concentrations ($1x10^{-4}$, $5x10^{-4}$, $1x10^{-3}$, $5x10^{-3}$, $1x10^{-2}$, and $5x10^{-2}$) mol/l and temperatures (298, 308, 318, and 328) K. The well-known equilibrium model of Langmuir and Freundlich is employed in this work. The Langmuir model predicts a homogeneous distribution of adsorbate on the adsorbent's surface, as well as an energetically similar monolayer or single layer of adsorption sites, with no interaction between adsorbed ions even at adjacent sites [29]. Freundlich isotherm model expression defines surface heterogeneity as well as the exponential distribution of active sites and active site energies [30]. The linear form of Langmuir equation and separation factor are given by following equations [29]:

$$\frac{C_e}{q_e} = \frac{C_e}{q_m} + \frac{1}{K_L q_m} \quad (3)$$

$$R_L = \frac{1}{1+K_L C_o} \quad (4)$$

Where, C_e is equilibrium concentration of adsorbate (mol/l), q_e is the amount of material adsorbed per gram of the adsorbent at equilibrium (mol/g), K_L Langmuir adsorption isotherm constant (l/mol), and q_m is maximal capacity of the mono-layer coverage (mol/g). The slope and intercept of the plot between C_e/q_e versus C_e will give q_m and K_L respectively as shown in

Figure 8. These results were similar to those obtained by Belbachir and Makhoukhi [31]. While the Langmuir constants K_L and Co initial Co (II) concentration were entered into Equation (4) to compute the separation constant R_L, which was found to be in the favorable range ($0<R_L<1$), indicating that Co (II) adsorption onto CS is advantageous.
The isothermal model of Freundlich adsorption is represented as follows [32]:

$$logq_e = logK_F + \frac{1}{n} logC_e \quad (5)$$

Where, q_e is the amount of material adsorbed per gram of the adsorbent at equilibrium (mol/g), C_e is equilibrium concentration of adsorbate (mol/l), K_F the adsorption capacity constant (mol/g), 1/n the adsorption intensity of the adsorbate towards the adsorbent or heterogeneity. The slope and intercept of the plot between log q_e versus log C_e will give 1/n and K_F respectively as shown in Fiqure 9. When 1/n = 1, the partition between the two phases is concentration independent. When the value of 1/n is less than one, this indicates (a normal adsorption). When 1/n values are greater than one, this indicates (a cooperative adsorption) [33,34]. The data in Table 2 show the adsorption of Co (II) on CS follows the Freundlich model (R^2 =0.937).

Table 2- Isotherms constants and correlation coefficient

Temp. (K)	Lanqmuir isotherm			Freundlich isotherm		
	K_L (l/mol)	q_m(mol/g)	R^2	K_F (mol/g)	1/n	R^2
298	2385.4	$103*10^{-5}$	0.477	271643.9	2.154	0.880
308	3604.9	$73*10^{-5}$	0.704	1153453.2	2.269	0.937
318	6438.3	$44*10^{-5}$	0.916	3318944.5	2.298	0.813
328	6624.2	$68*10^{-5}$	0.748	1874994.5	2.189	0.880

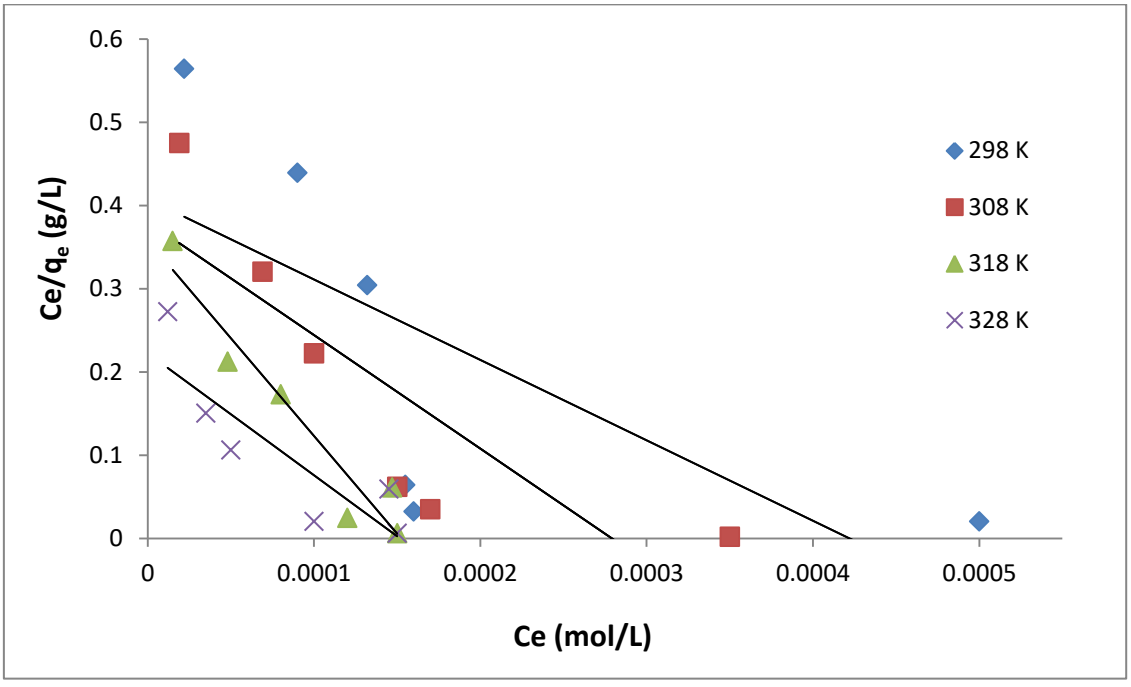

Figure 8- Langmuir adsorption isotherm of Co (II) onto CS.

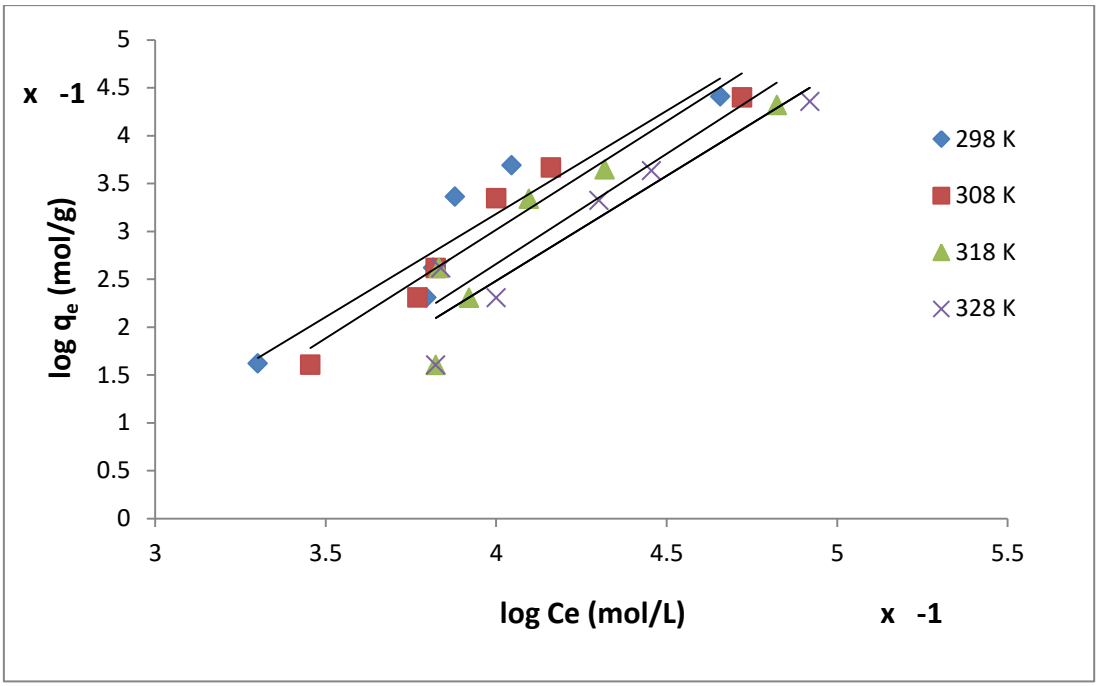

Figure 9- Freundlich adsorption isotherm of Co (II) onto CS.

3.7. Adsorption Kinetics

In order to better understand the adsorption process, kinetics of adsorption and adsorption process control mechanisms are highlighted and crucial for designing the time and rate of adsorption. [29,35]. There are few adsorptions kinetic models such as pseudo-first order and pseudo-second order. The linear form of pseudo-first order is expressed as follows [36]:

$$\log(q_e - q_t) = log\, q_e - \frac{k_1}{2.303} t \quad (6)$$

Where, k_1 is pseudo-first order rate constant for the adsorption process (min^{-1}) q_e and q_t is the amount of adsorbed (mol/g) at equilibrium and at the time t (min). The slope and intercept of the plot between log (q_e-q_t) versus t will give k_1 and q_e respectively as shown in Fiqure 10.
A pseudo-second order equation can be presented in a linear form as follows [37]:

$$\frac{t}{q_t} = \frac{1}{k_2 q_e^2} + \frac{t}{q_e} \quad (7)$$

Where, k_2 is the equilibrium rate constant of the pseudo-second order sorption (g/mol min). The slope and intercept of the plot between t/q_t versus t will give q_e and k_2 respectively. The following equation relates the initial adsorption rate h_o at different initial concentrations [38]:

$$h_o = k_2 q_e^2 \quad (8)$$

The comparison of kinetic constants and correlation coefficients of kinetic models shows that the pseudo-second order model fits better, as shown in Table 3.

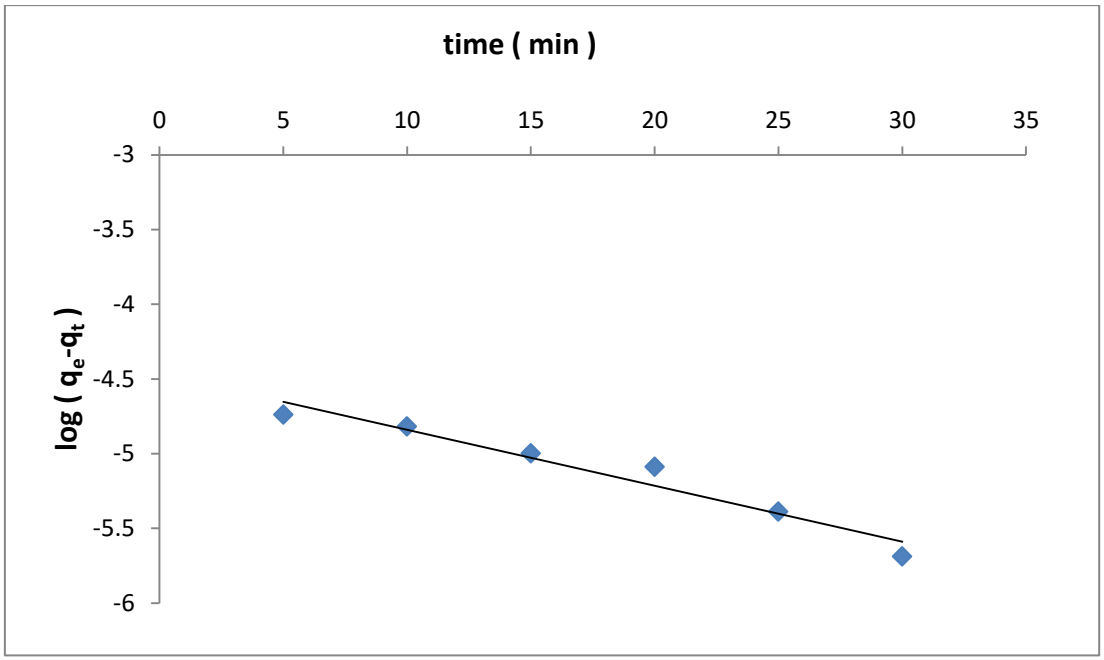

Figure 10- Pseudo-first order of Co (II) onto CS at 298K.

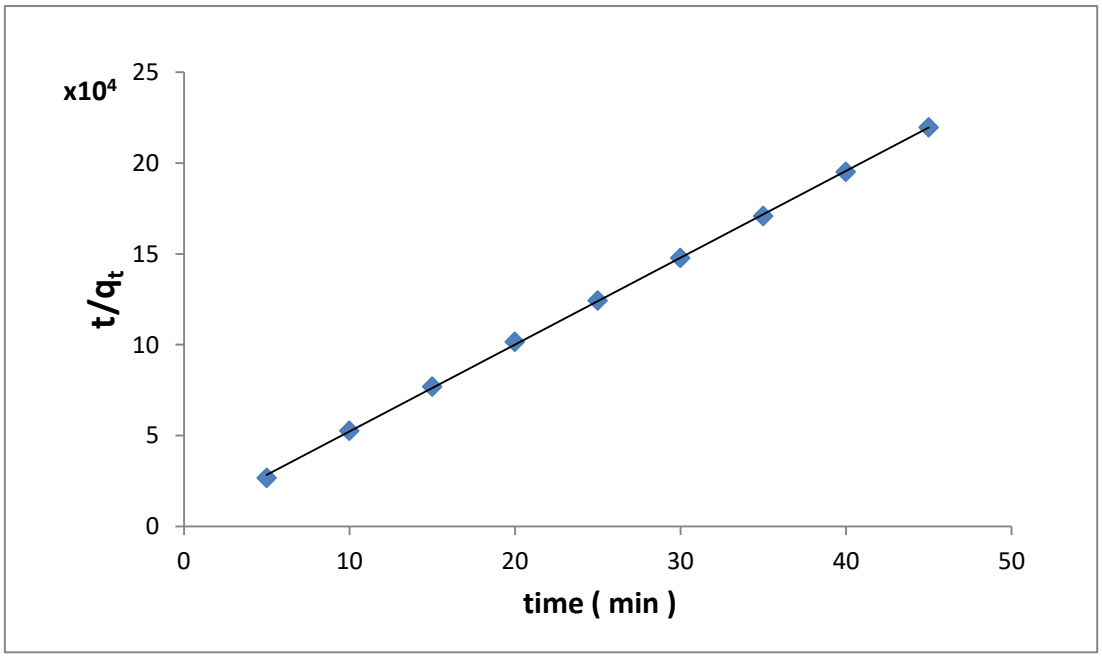

Figure 11- Pseudo-second order of Co (II) onto CS at 298K.

Table 3- Kinetic results of $5x10^{-4}$ mol/l Co (II) on CS at 298K

$q_{e,exp.}$ (mol/g)	Pseudo-first order			Pseudo-second order		
	k_1 (min^{-1})	$q_{e,cal}$ (mol/g)	R^2	k_2 (g/mol.min)	$q_{e,cal}$(mol/g)	R^2
$205x10^{-6}$	0.037	$34x10^{-6}$	0.946	5174.78	$209x10^{-6}$	0.999

3.8. Thermodynamic studies

Thermodynamic parameters are calculated by following equations [38]:

$$K_c = \frac{C_{ads}}{C_e} = \frac{C_o - C_e}{C_e} = \frac{C_o}{C_e} - 1 \quad (9)$$

$$\Delta G^o = -RTlnK_c \quad (10)$$

$$lnK_c = \frac{\Delta S^o}{R} - \frac{\Delta H^o}{RT} \quad (11)$$

Where, C_o the original Co(II) concentration (mol/l), K_c equilibrium constant, C_e remaining concentration in solution at equilibrium (mol/l) and C_{ads} concentration of adsorbed cobalt (mol/l). ΔG^o The change in the Gibbs free energy, ΔS^o the entropy and ΔH^o enthalpy. T(K) solution absolute temperature and R gas constant (8.314 $J.mol^{-1}.K^{-1}$). The slope and intercept of the Van't Hoff plot (Figure12) are used to compute ΔH^o and ΔS^o, and the ΔG^o has a negative value, indicating that the adsorption of Co (II) onto CS was spontaneous. Table 4 summarizes the thermodynamic results, which show that a positive entropy value indicates an increase in randomness and a positive enthalpy value indicates that the adsorption reaction was endothermic.

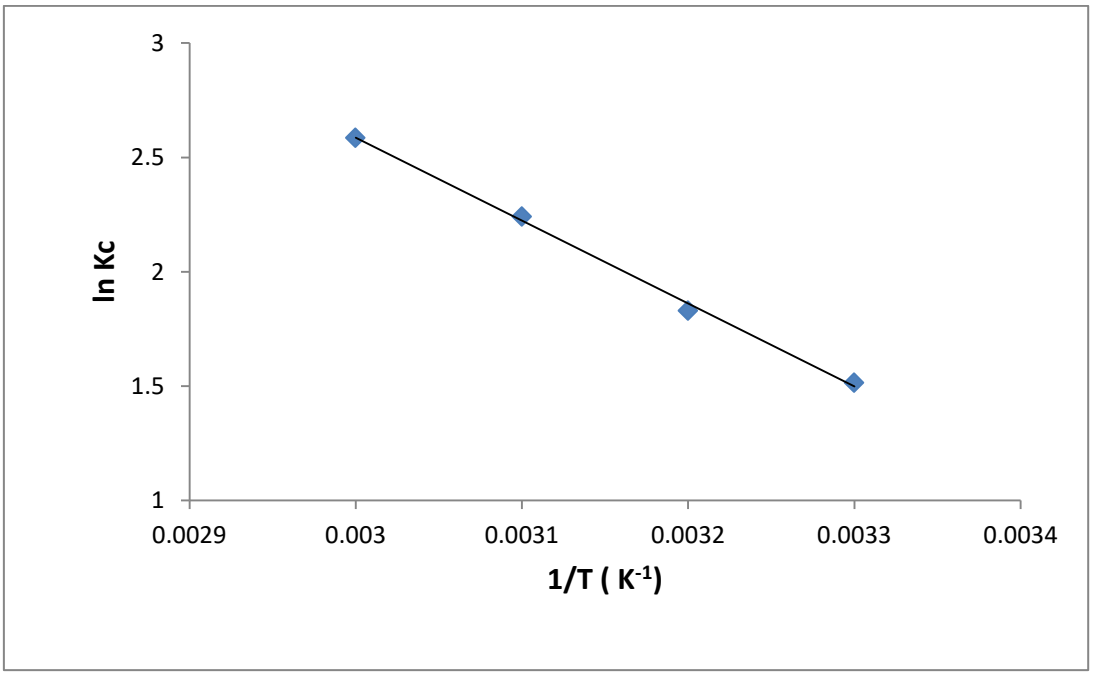

Figure 12-Van't Hoff plot of Co (II) onto CS.

Table 4- Values of thermodynamic parameters for the adsorption of Co (II) onto CS

T(K)	ΔG^o (KJ/mol)	ΔH^o (KJ/mol)	ΔS^o (KJ/mol.K)
298	-3.753	+30.129	+0.111
308	-4.688		
318	-5.926		
328	-7.052		

4. Conclusions

The Co (II) was successfully removed from industrial effluent using a natural chitosan adsorbent. The Langmuir and Freundlich models were employed to characterize adsorption isotherms, with the Freundlich model offering the greatest match for equilibrium data. The adsorption process appears to be endothermic and spontaneous, according to thermodynamic studies.

References

[1] K. Y. Hor *et al.*, "Evaluation of physicochemical methods in enhancing the adsorption performance of natural zeolite as low-cost adsorbent of methylene blue dye from wastewater," *J. Clean. Prod.*, vol. 118, pp. 197–209, 2016.

[2] C. Dong, J. Lu, B. Qiu, B. Shen, M. Xing, and J. Zhang, "Developing stretchable and graphene-

oxide-based hydrogel for the removal of organic pollutants and metal ions," *Appl. Catal. B Environ.*, vol. 222, no. October 2017, pp. 146–156, 2018.

[3] J. H. Kim, H. J. Gibb, and P. Howe, *Cobalt and inorganic cobalt compounds*, no. 69. World health organization, 2006.

[4] C. Cojocaru, G. Zakrzewska-Trznadel, and A. Jaworska, "Removal of cobalt ions from aqueous solutions by polymer assisted ultrafiltration using experimental design approach. part 1: Optimization of complexation conditions," *J. Hazard. Mater.*, vol. 169, no. 1–3, pp. 599–609, 2009.

[5] S. A. El-Safty, M. R. Awual, M. A. Shenashen, and A. Shahat, "Simultaneous optical detection and extraction of cobalt (II) from lithium ion batteries using nanocollector monoliths," *Sensors Actuators B Chem.*, vol. 176, pp. 1015–1025, 2013.

[6] G. Z. Kyzas, E. A. Deliyanni, and K. A. Matis, "Activated carbons produced by pyrolysis of waste potato peels: Cobaltions removal by adsorption," *Colloids Surfaces A Physicochem. Eng. Asp.*, vol. 490, pp. 74–83, 2016,

[7] D. Citak and M. Tuzen, "A novel preconcentration procedure using cloud point extraction for determination of lead, cobalt and copper in water and food samples using flame atomic absorption spectrometry," *Food Chem. Toxicol.*, vol. 48, no. 5, pp. 1399–1404, 2010.

[8] M. R. Awual *et al.*, "Inorganic-organic based novel nano-conjugate material for effective cobalt (II) ions capturing from wastewater," *Chem. Eng. J.*, vol. 324, pp. 130–139, 2017.

[9] C. Y. Cheang and N. Mohamed, "Removal of cobalt from ammonium chloride solutions using a batch cell through an electrogenerative process," *Sep. Purif. Technol.*, vol. 162, pp. 154–161, 2016.

[10] V.-P. Dinh *et al.*, "Determination of cobalt in seawater using neutron activation analysis after preconcentration by adsorption onto γ-MnO2 nanomaterial," *J. Chem.*, vol. 2018, 2018.

[11] S. A. Khan, Z. Uddin, and Z. A. Ihsanullah, "Levels of selected heavy metals in drinking water of Peshawar City," *Int J Sci Nat*, vol. 2, no. 3, pp. 648–652, 2011.

[12] F. Fu and Q. Wang, "Removal of heavy metal ions from wastewaters: A review," *J. Environ. Manage.*, vol. 92, no. 3, pp. 407–418, 2011, doi: 10.1016/j.jenvman.2010.11.011.

[13] E. Bazrafshan, L. Mohammadi, A. Ansari-Moghaddam, and A. H. Mahvi, "Heavy metals removal from aqueous environments by electrocoagulation process - A systematic review," *J. Environ. Heal. Sci. Eng.*, vol. 13, no. 1, 2015.

[14] C. F. Carolin, P. S. Kumar, A. Saravanan, G. J. Joshiba, and M. Naushad, "Efficient techniques for the removal of toxic heavy metals from aquatic environment: A review," *J. Environ. Chem. Eng.*, vol. 5, no. 3, pp. 2782–2799, 2017.

[15] A. Li *et al.*, "An environment-friendly and multi-functional absorbent from chitosan for organic pollutants and heavy metal ion," *Carbohydr. Polym.*, vol. 148, pp. 272–280, 2016.

[16] I. Younes and M. Rinaudo, "Chitin and chitosan preparation from marine sources. Structure, properties and applications," *Mar. Drugs*, vol. 13, no. 3, pp. 1133–1174, 2015.

[17] A. Sumaila, M. M. Ndamitso, Y. A. Iyaka, A. S. Abdulkareem, J. O. Tijani, and M. O. Idris, "Extraction and Characterization of Chitosan from Crab Shells: Kinetic and Thermodynamic Studies of Arsenic and Copper Adsorption from Electroplating Wastewater," *Iraqi J. Sci.*, pp. 2156–2171, 2020.

[18] G. Rojas, J. Silva, J. A. Flores, A. Rodriguez, M. Ly, and H. Maldonado, "Adsorption of chromium onto cross-linked chitosan," *Sep. Purif. Technol.*, vol. 44, no. 1, pp. 31–36, 2005.

[19] R. Ahmad and R. Kumar, "Adsorption studies of hazardous malachite green onto treated ginger waste," *J. Environ. Manage.*, vol. 91, no. 4, pp. 1032–1038, 2010.

[20] K. Zhang, R. Hu, G. Fan, and G. Li, "Graphene oxide/chitosan nanocomposite coated quartz crystal microbalance sensor for detection of amine vapors," *Sensors Actuators, B Chem.*, vol. 243, pp. 721–730, 2017.

[21] R. S. C. M. de Queiroz Antonino *et al.*, "Preparation and Characterization of Chitosan Obtained from Shells of Shrimp (Litopenaeus vannamei Boone)," *Mar. Drugs*, vol. 15, no. 5, p. 141, May 2017.

[22] K. Okuyama, K. Noguchi, T. Miyazawa, T. Yui, and K. Ogawa, "Molecular and crystal structure of hydrated chitosan," *Macromolecules*, vol. 30, no. 19, pp. 5849–5855, 1997.

[23] A. Kucukgulmez, M. Celik, Y. Yanar, D. Sen, H. Polat, and A. E. Kadak, "Physicochemical

characterization of chitosan extracted from Metapenaeus stebbingi shells," *Food Chem.*, vol. 126, no. 3, pp. 1144–1148, 2011.

[24] P. Dhawade and R. N. Jagtap, "Characterization of the glass transition temperature of chitosan and its oligomers by temperature modulated differential scanning calorimetry," *Adv Appl Sci Res*, vol. 3, pp. 1372–1382, Jan. 2012.

[25] A. Farhan, R. Jassim, and N. Kadhim, "The Removal of Zinc from Aqueous Solutions Using Malvaparviflora," *Baghdad Sci. J.*, vol. 13, no. 3, pp. 482–488, 2016.

[26] K. A. Kareem, "Removal and Recovery of Methylene Blue Dye from Aqueous Solution using Avena Fatua Seed Husk," *ibn Al-Haitham J. Pure Appl. Sci.*, vol. 29, no. 3, pp. 179–194, 2016.

[27] S. Sonawane, P. Chaudhari, S. Ghodke, S. Phadtare, and S. Meshram, "Ultrasound assisted adsorption of basic dye onto organically modified bentonitenanoclay," *J. Sci. Ind. Res. (India).*, vol. 68, no. 2, pp. 162–167, 2009.

[28] M. Rafatullah, O. Sulaiman, R. Hashim, and A. Ahmad, "Adsorption of copper (II), chromium (III), nickel (II) and lead (II) ions from aqueous solutions by meranti sawdust," *J. Hazard. Mater.*, vol. 170, no. 2–3, pp. 969–977, 2009.

[29] M. T. Yagub, T. K. Sen, S. Afroze, and H. M. Ang, "Dye and its removal from aqueous solution by adsorption: A review," *Adv. Colloid Interface Sci.*, vol. 209, pp. 172–184, 2014.

[30] M. A. Al-Ghouti and D. A. Da'ana, "Guidelines for the use and interpretation of adsorption isotherm models: A review," *J. Hazard. Mater.*, vol. 393, no. November 2019, p. 122383, 2020.

[31] I. Belbachir and B. Makhoukhi, "Adsorption of Bezathren dyes onto sodic bentonite from aqueous solutions," *J. Taiwan Inst. Chem. Eng.*, vol. 75, pp. 105–111, 2017.

[32] L. Liu, X. B. Luo, L. Ding, and S. L. Luo, *Application of Nanotechnology in the Removal of Heavy Metal From Water*. Elsevier Inc., 2018.

[33] D. A.O, "Langmuir, Freundlich, Temkin and Dubinin–Radushkevich Isotherms Studies of Equilibrium Sorption of Zn 2+ Unto Phosphoric Acid Modified Rice Husk," *IOSR J. Appl. Chem.*, vol. 3, no. 1, pp. 38–45, 2012.

[34] A. B. D. Nandiyanto *et al.*, "Adsorption Isotherm of Carbon Microparticles Prepared from Pumpkin (Cucurbita maxima) Seeds for Dye Removal," *Iraqi J. Sci.*, pp. 1404–1414, 2021.

[35] J. Y. Lim, N. M. Mubarak, E. C. Abdullah, S. Nizamuddin, M. Khalid, and Inamuddin, "Recent trends in the synthesis of graphene and graphene oxide based nanomaterials for removal of heavy metals — A review," *J. Ind. Eng. Chem.*, vol. 66, pp. 29–44, 2018.

[36] E. . M. Al-kinani, "Studies on Removal of Hexavalent Chromium Ion from Aqueous Solution Using Polyaniline Composite," *J. Al-Nahrain Univ.*, vol. 19, no. 2, pp. 58–68, 2016.

[37] Y.-S. Ho and G. McKay, "Pseudo-second order model for sorption processes," *Process Biochem.*, vol. 34, no. 5, pp. 451–465, 1999.

[38] K. A. Al-Rudaini, "Adsorption Removal of Rhodamine-B Dye from Aqueous Solution Using Rhamnus Stone as Low Cost Adsorbent," *J. Al-Nahrain Univ.*, vol. 20, no. 1, pp. 32–41, 2017.